engineering proceedings

MDPI

Proceeding Paper

Failure Analysis of API 5L Grade B Underground Crude Oil Transfer Pipe †

Mujiono * and Fahmi Mubarok

Mechanical Engineering Department, Sepuluh Nopember Institute of Technology, Sukolilo, Surabaya 60111, Indonesia; fmubarok@gmail.com

* Correspondence: muji.me09@gmail.com

† Presented at the 7th Mechanical Engineering, Science and Technology International Conference, Surakarta, Indonesia, 21–22 December 2023.

Abstract: An underground transfer pipe was utilized to deliver crude oil from the BDA gathering station to the A main gathering station. The transfer pipe made of API 5L grade B has a diameter of 6 inches and a length of 18,000 m. The pipe has a design life of 20 years, but after being operated for five years, 41 points of leakage were found in the area of KM 14 to KM 16. Visual inspection of the leakages in the pipe indicates general corrosion as the main issue. Nevertheless, failure analysis is required to investigate the root cause of the problem in this area. Several characterization methods were performed, including ultrasonic testing, to measure the distribution of pipe thickness. SEM and EDS testing were conducted to understand the hole formations that led to leakage and study their elemental changes around the leakage point. XRD and FTIR characterization were carried out on the deposit found on the inner diameter of the pipe. The ultrasonic thickness measurement indicates gradual pipe thinning until a hole was formed. Deposit analysis revealed wax composition at the upper level of the pipe formed due to transferred crude oil, while the bottom deposit where leakage was identified consisted of corrosion products such as FeO_2 (geothite), Fe_2O_3 (hematite) and Fe_3O_4 (magnetite). The leakage failure in KM 14 and KM 16 was discovered to be where the pipe was at its lowest elevation point of underground pipe installation. This situation causes the pipe to be submerged by produced water at the 3 o'clock to 9 o'clock position, which initiates the occurrence of oxygen-influenced corrosion and the formation of hydroxide ions (OH^-). The formation of hydroxide ions (OH^-) triggers the Under Deposit Corrosion (UDC) mechanism.

Keywords: corrosion; oil; pipe

check for updates

Citation: Mujiono; Mubarok, F. Failure Analysis of API 5L Grade B Underground Crude Oil Transfer Pipe. *Eng. Proc.* **2024**, *63*, 29. https://doi.org/10.3390/engproc2024063029

Academic Editor: Agus Dwi Anggono

Published: 27 May 2024

Copyright: © 2024 by the authors. Licensee MDPI, Basel, Switzerland. This article is an open access article distributed under the terms and conditions of the Creative Commons Attribution (CC BY) license (https://creativecommons.org/licenses/by/4.0/).

1. Introduction

Oil, water and natural gas from a well flow through pipes to the separator in a gathering station (GS). In the separator, gas and liquid are separated. The gas then flows to the consumer, while the liquid fluid in the form of oil and water is transferred to the main gathering station (MGS) via a transfer pipe. After arriving at the main gathering station, the oil and water are separated through a separator. The oil is then distributed to the processing plant, while the separated water is treated before being reinjected into the injection well. The transfer pipe from the BDA gathering station (BDA GS) to the A main gathering station (A MGS) functions to distribute crude oil with water cut 50%, with a pipe length of 18,000 m, the majority of which is buried underground. The pipe began operating in December 2014 with a design life of 20 years. In January 2021 leaks began to occur and in the period January 2021 to July 2022 there were 41 leaks. With the rapid growth of demand for petroleum and gas, an increasing number of underground pipelines have been constructed to transport oil and natural gas resources [1].

A leak is indicated by the release of fluid on the ground surface and then temporary clamping is carried out as in Figure 1. The leak points are spread between KM 14 and KM 16.

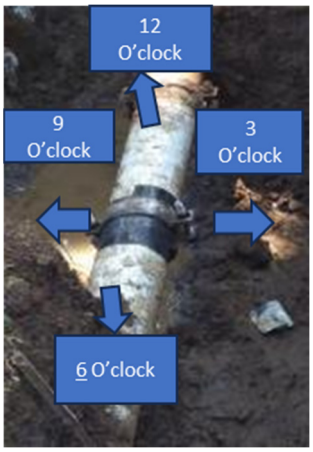

Figure 1. Pipe leak condition after temporary clamping is carried out.

When there is a pipe leak, excavation is carried out for temporary clamping. When installing the clamping, it was discovered that the leak point was at the bottom of the pipe with an orientation of 4 to 8 o'clock and thus initiated general corrosion. There were indications that, at this position, the flowing fluid had a lot of water content. This can be seen in the excavation hole when carrying out a temporary clamp, as shown in Figure 2.

Figure 2. Water out of the leak.

A pipeline system is said to be suitable for transportation of large quantities of oil and gas because there is relative freedom from impacts of weather conditions [2]. The main reason for the operation of oil pipelines is the corrosion of their materials. As a result of corrosion, the destruction of the pipeline, contributing to the leakage of oil, which pollutes the environment, causes accidents and disasters [3]. Corrosion costs of the oil industry are billions of dollars a year [4]. Pipeline corrosion is a quite complex phenomenon, and the complexity arises as a result of the interaction of multiple reactions and processes occurring simultaneously, which in turn are very specific to both the material and the environmental interaction [5]. Corrosion occurs as an electrochemical reaction [6]. Corrosion refers to the destructive reaction of a metal with its environment. It takes place in the presence of a supportive medium, which is referred to as an electrolyte [7].

Corrosion in pipelines is one of the significant challenges faced in the oil and gas industries all over the world. Corrosion is a natural process, which converts a refined metal to a more chemically stable form, such as its oxide, hydroxide or sulfide [8]. Specifically, a large portion of carbon steel pipes is buried underground, and the corrosion behavior can be affected by different factors, e.g., temperature, pressure, concentrations of corrosive

species, flow rate of the fluid around the pipes, etc. Extensive research has been focused on the effects of various factors on the corrosion mechanism of carbon steel pipes in service [9].

The flow regime may cause accumulation of water at pipeline low spots or, depending on the product type, accumulation of water-wetted solid particles at the pipeline bottom, typically downstream of over-bends, thereby forming corrosion "hotspots" [10]. The transfer pipe from BDA Gathering Station to Main Gathering Station A is in an underground position with varying heights above sea level. Fluids flow from BDA Gathering Station which has a higher elevation (30 MASL) to Main Gathering Station A which has a lower elevation (11 MASL). Pipe elevation data are obtained from the as-built drawing, as shown in Figure 3.

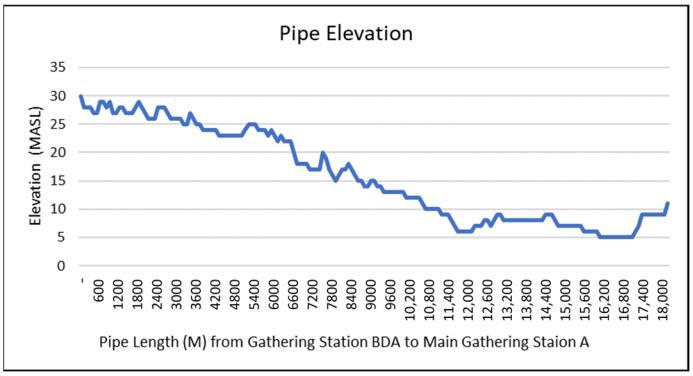

Figure 3. Transfer pipe elevation.

2. Experimental Method

Experimental method failure analysis crude oil transfer pipe see Figure 4.

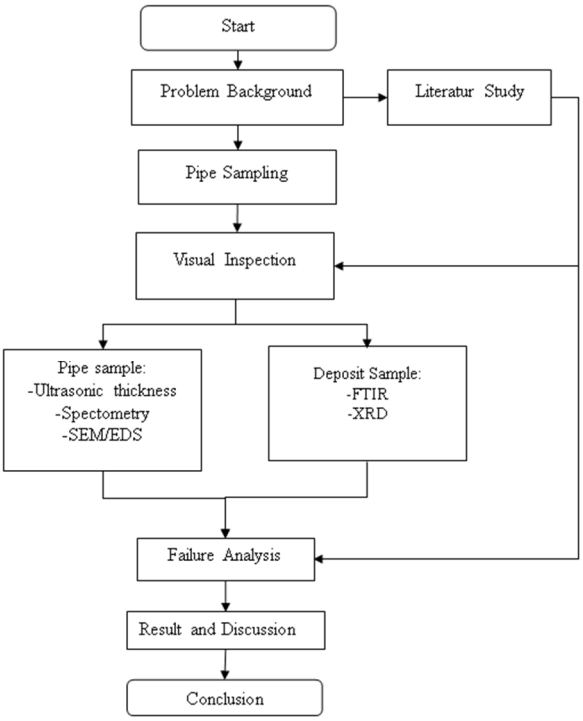

Figure 4. Experimental Method Failure Analysis Crude Oil Transfer Pipe.

2.1. Pipe Sampling

Pipe sampling was carried out on the transfer pipe, which experienced a leak at kilometre 14. The condition of the underground pipe was such that excavation was carried

out before cutting using a cutting torch. After excavation, a mark was made on the top of the pipe to ensure the clock direction of the pipe leak as shown in Figure 5a. After the pipe sample was lifted to the surface, the pipe was taken to the workshop with the temporary clamp still attached as shown in Figure 5b. The temporary clamping was released to see the leak point as shown in Figure 5c. It can be seen that the position of the pipe leak was uniform and tended to occur in a straight line, namely at the bottom of the 4 to 8 o'clock transfer pipe. The pipe was cut using a cold cutting machine (Figure 5d) at the yellow line position (Figure 5c).

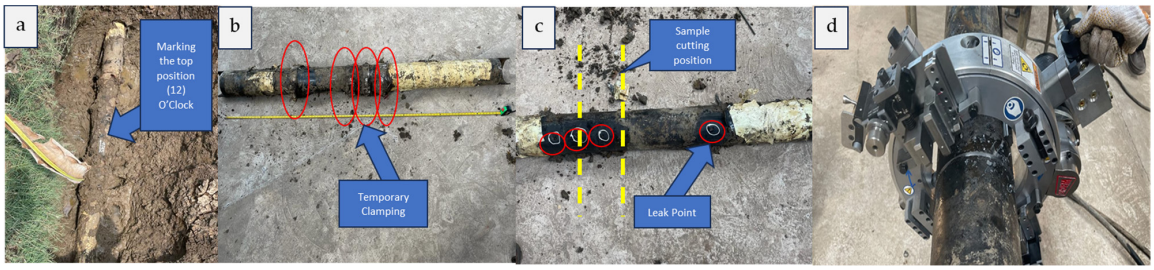

Figure 5. Pipe sampling. (**a**) Marking on pipe samples before cutting; (**b**) Temporary clamping; (**c**) Sample cutting position; (**d**) Sample cutting.

An OEM spectrometry SpectroMaxx metal analyzer, from SPECTRO Analytical Instruments GmbH, Kleve, Germany was used to analyze the chemical composition of the API 5L grade B. Ultrasonic testing using GE Inspection Technologies DM4 DL From New York, NY, USA with accuracy 0.01 mm was carried out to measure the thickness distribution. FTIR testing was carried out using Thermo Fisher Scientific, Waltham, MA, USA with a set up of region 400–4000, absolute threshold 95.457, and sensitivity 50.

2.2. Visual Observations

Visual observations are carried out to see pipe leaks directly. Observations are made at the point of the leak, the position of the leak when the pipe is installed, the shape of the leak, the presence of deposits, the shape of the deposit, and the colour of the deposit.

2.3. X-ray Diffraction (XRD) and Fourier Transform Infrared (FTIR)

XRD and FTIR characterization were conducted on the deposit found on the inner diameter of the pipe.

2.4. SEM and EDS

SEM and EDS testing were conducted to understand the hole formations that led to leakage and study their elemental changes around the leakage point.

2.5. Corrosion Rate

Based on API 570, the pipeline corrosion rate can be calculated using the following formula [11]:

$$\text{Corrosion Rate (LT)} = \frac{t_{initial} - t_{actual}}{\text{time (year) between } t_{initial} \text{ and } t_{actual}} \quad (1)$$

Corrosion Rate (LT): long term corrosion rate (mm) per year;
$t_{initial}$: thickness at the same point during installation (mm);
t_{actual}: actual thickness at the time of inspection (mm).

3. Result and Discussion

After taking the sample, it was discovered that there was sediment in the pipe. The deposits on the inside of the upper pipe were shaped like wax, while the deposits on the inside of the lower pipe were shaped like a scale as shown in Figure 6.

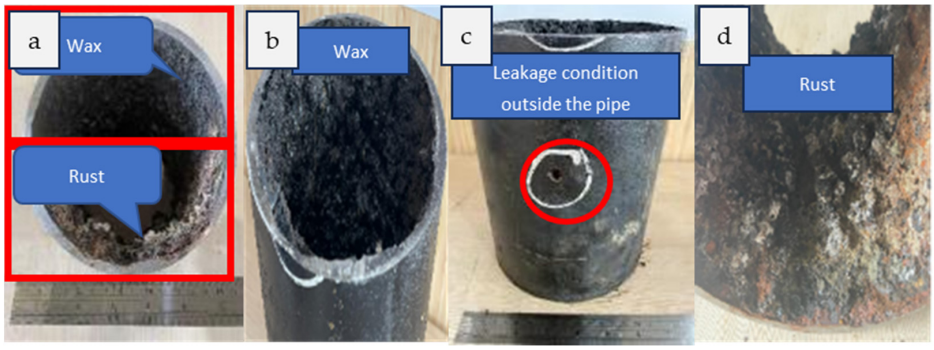

Figure 6. Visual Inspection. (**a**) Visual inspection of samples; (**b**) Visual inspection of wax; (**c**) Leakage condition outside the pipa; (**d**) Visual inspection of rust.

Wax deposition in oil–water stratified flows is commonly encountered in onshore and offshore oil-production pipe systems, and typically reduces transportation capacity of oil [12]. Deposition and transformation of molecules of wax into a wax gel that occupies the cross-section area of a pipeline's inner surface occur when the bulk oil temperature (BOT) falls below the wax appearance temperature (WAT). The effective surface area for fluid flow is reduced as a result of deposition of untreated wax, and in extreme scenarios completely blocks the pipeline which eventually leads to complete production shutdown and huge financial loss to the oil and gas sector [13].

From visual inspection, it can be seen that there is no visible corrosion on the outside of the pipe. Corrosion that occurs in the crude oil transfer pipe from Gathering Station BDA to Main Gathering Station A occurs on the inside of the pipe as shown in Figure 7.

Figure 7. Pipe hole position (in red circle) after cleaning deposits. (**a**) View of the hole from inside the pipe; (**b**) view of the hole from outside the pipe; (**c**) Detail a.

The crude oil transfer pipeline from Gathering Station BDA to Main Gathering Station A began operating in December 2014 using a new condition pipe with a diameter of 6 inches (Schedule 40), which has a new pipe wall thickness of at least 7.11 mm. In January 2021, a leak started to occur; the pipe wall thickness was 0 mm. The pipe corrosion rate is as follows:

$$\text{Corrosion Rate (LT)} = \frac{t_{initial} - t_{actual}}{\text{time (year) between } t_{initial} \text{ and } t_{actual}} \quad (2)$$

$$\text{Corrosion Rate (LT)} = \frac{7.11 \text{ mm} - 0 \text{ mm}}{5.083 \text{ year}} \quad (3)$$

$$\text{Corrosion Rate (LT)} = 1.3987 \text{ mm per year} \quad (4)$$

The corrosion rate of 1.3987 mm per year is higher than the pipe design corrosion rate of 0.1016 mm per year. It can be concluded that the corrosion rate that occurred was 13.77 times faster than the design corrosion rate.

At the pipe length points KM 11.2 to KM 16.8, there is a pipe elevation at the lowest point, 5 to 9 m above sea level (MASL). At the end of the pipe at KM 18, there is an increase in pipe elevation so that when pumping stops, the fluid in the pipe cannot be flushed, so the fluid is stuck in the pipe. This causes sediment to form in the pipe due to the fluid being stationary for 7 to 9 h per day.

The fluid in the transfer pipe consists of crude oil and water, so laboratory tests are carried out on crude oil fluid and water fluid. Crude oil laboratory data can be seen in Table 1 and water labolatory data are shown in Table 2.

Table 1. Crude oil laboratory test results.

No	Parameter	Result	Unit
1	Obs Density	864.4/28 °C	kg/m^3
2	Density 15 °C	873.3	kg/m^3
3	Spesific Gravity 60/60 °F	0.8738	-
4	API Gravity 60 °F	30.44	-
5	Viskositas kinematik pada 100 °F	74.842	mm^2/s
6	Viskositas kinematik pada 122 °F	56.383	mm^2/s
7	Viskositas kinematik pada 140 °F	46.554	mm^2/s
8	Pour Point	24	°C
9	Flash Point	28	°C
11	Sulphur Content	0.2535	% berat
12	Salt Content	23.4	Ptb

Table 2. Water produced laboratory test result.

No	Parameter	Result (BDA)	Result (MGS A)	Unit
1	Ph	8.45	8.5	-
2	Suspended Solid (1.5 mikron)	22.75	15	mg/L
3	Dissolved Oxygen	3.96	1.37	ppm
4	CO_2	0	0	mg/L
5	SRB (Sulfate-Reducing Bacteria)	10^3–10^4	$<10^1$	
6	Calcium (Ca^{2+})	135.470	156.713	mg/L
7	Magnecium (Mg^{2+})	39.642	41.83	mg/L
8	Ferum Rotal (Fe^{3+})	0.130	0.38	mg/L
9	Natrium (Na+)	6721	6789	mg/L
10	Chloride (Cl^-)	9968	10,043	mg/L
11	Bicarbonat ($HCO_3{}^{2-}$)	1.116	1128	mg/L
12	Carbonate ($CO_3{}^{2-}$)	93.016	150.025	mg/L
13	Hydroxide (OH^-)	0	0	mg/L
14	Sulfate ($SO_4{}^{2-}$)	5	5	mg/L

From Table 1, it can be seen that the crude oil flowing in the pipe has a specific gravity of 0.8738, which means it is lower than the specific gravity of water. Crude oil has a pour point at a temperature of 24 °C or 75.2 °F, which means that the oil is a High Pour Point Oil (HPPO) type. HPPO oil has a pour point ranging from 60 to 125 °F [14]. Formation water testing showed the presence of sulphate-reducing bacteria (SRB) in BDA Gathering Station amounting to 10^3–10^4 and in A Gathering Station amounting to $<10^1$. The optimal temperature for SRB growth is 40–110 °F (25–43 °C), with a maximum temperature limit of 120 °F (49 °C). The temperature of the formation water and crude oil at the BDA Gathering Station is >141 °F (60 °C), so at this temperature SRB cannot develop. The conclusion of observations of corrosion that occurred on transfer pipe BDA Gathering Station to Main

A Gathering Station was that there was thinning corrosion. There was no visible pitting corrosion as is characteristic of corrosion caused by SRB. So it was concluded that the corrosion that occurred was not caused by SRB. From Table 2, it can be seen that the formation water flowing in the pipe at the BDA Gathering Station dissolved oxygen of 3.96 ppm, and at the A Main Gathering Station it decreased to 1.37 ppm. There was a decrease in the dissolved oxygen value after the water flowed into the pipe. There was a possibility that oxygen reacted in the pipe. From Table 2, it can also be seen that the water flowing in the pipe did not contain CO_2, so corrosion in the pipe was not caused by CO_2. The results of the produced water test showed that there was a chloride (Cl^-) content of 9968 mg/L at the GS BDA and 10,043 mg/L at the MGS A. Chloride content can cause under-deposit corrosion.

Wall thickness measurements were carried out on the pipe diameter circle, which contained 36 leak points in positions as shown in Figure 8. From the measurement results, it can be seen that the position of the inside of the upper side pipe does not experience much thinning with a thickness of 7 mm. Meanwhile, the inside position of the bottom side of the pipe experienced thinning with a pipe thickness of up to 0.5 mm. This thinning occurs in areas where there are deposits in the form of rust.

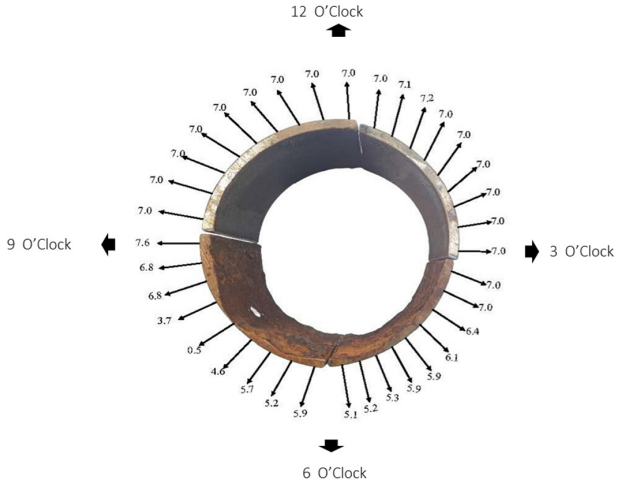

Figure 8. Wall Thickness.

Spectrometry test results can be seen in Table 3. From the test, it can be confirmed that the crude oil transfer pipe from BDA to MGS A is an API 5L Grade B pipe.

When protective iron carbonate scales form (typically at higher pH in produced water) or when inhibitor films are present on the steel surface, the above-mentioned effect of flow becomes insignificant as the main resistance to corrosion is now in the surface scale or inhibitor film. In this case, the effect of the flow is to interfere with the formation of surface scales/films or to remove them once they are in place, leading to an increased corrosion rate [15]. An X-ray Diffraction (XRD) test was carried out on deposit samples at the top of the pipe (Figure 9a) and at the bottom of the pipe (Figure 9b). In the XRD results, the deposits on the inside of the upper pipe could not be identified. The deposit was in the form of a wax crude oil aromatic phase, so FTIR testing (Figure 9c) was carried out to ensure that the deposit was a crude oil deposit. From XRD testing, it can be seen that the main elements of the deposit at the bottom of the pipe (Figure 9b) are FeO_2 (geothite), Fe_2O_3 (hematite), and Fe_3O_4 (magnetite), which are iron oxide. Iron oxide deposits can increase the risk of pipe failure. If FeO_2 covers the pipe area, it can cause local corrosion. Stretching absorption (Figure 9c) occurs when the wax experiences CH_3 asymmetric stretching at waves 2954.05 cm^{-1}, 2915.43 cm^{-1}, and 2847.48 cm^{-1}. At waves 1472.31 cm^{-1} and 1461.8 cm^{-1}, absorption band splitting deformation occurs; the band overlaps with the vibration scissor CH_2. At wave 1376.81 cm^{-1}, absorption band splitting deformation occurs, and CH_3 vibrations are symmetrical. At waves 728.78 cm^{-1} and

718.89 cm^{-1}, rocking absorption occurs when there are four or more CH_2 in a row with the type of aromatic compound. This proves that the crude oil flowing in the pipe is a type of heavy oil which has large amounts of sediment.

Table 3. Spectrometry Test.

Item No.	Heat No.	Material Testing Report									
			Chemical Composition								
			C %wt	Mn %wt	P %wt	S %wt	Ti %wt	Cr %wt	Mo %wt	Ni %wt	V %wt
		Min	0.0000	0.0000	0.0000	0.0000	0.0000	0.0000	0.0000	0.0000	
		Max	0.2800	1.2000	0.0300	0.0300	0.0400	0.0400	0.0400	0.0150	
1	Sample		0.0271	0.6360	0.0124	0.0045	0.0010	0.0262	0.0043	0.0098	0.003

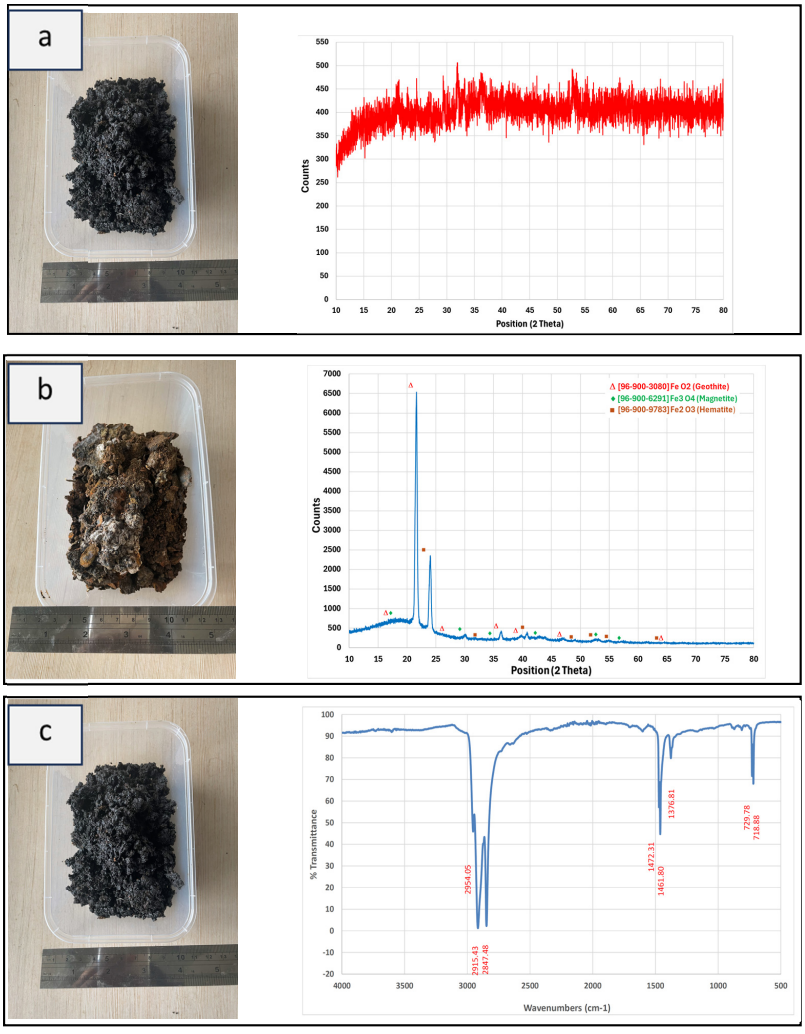

Figure 9. XRD and FTIR test result: (**a**) XRD test results of deposits in the upper pipe; (**b**) XRD test results of deposits in the lower pipe; (**c**) FTIR test results of deposits in the upper pipe.

SEM (Figure 10) testing was carried out on the bottom pipe sample where there was a pipe leak. From the SEM test results, it can be seen that the surface morphology of the pipe contained corrosion varies, with irregularities and smooth rod-like shapes with different directions.

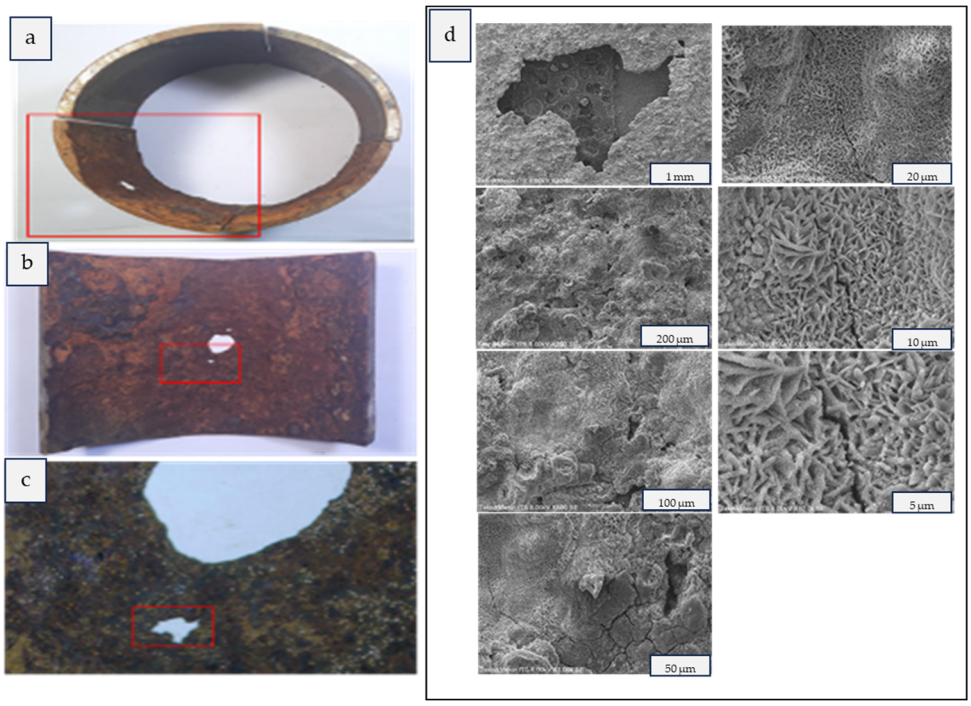

Figure 10. Scanning electron microscope (SEM) in red box area. (**a**) SEM pipe samples; (**b**) Detail a; (**c**) Detail b; (**d**) SEM test results.

Energy Dispersive Spectrometer (EDS) is a method used to determine the elements contained in a sample with the following results (Figure 11):

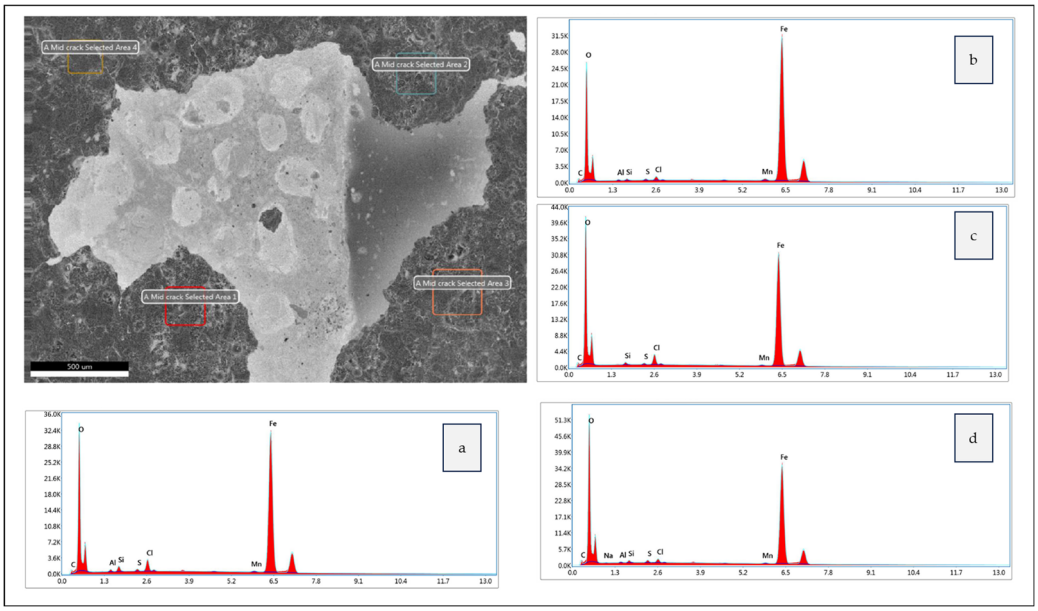

Figure 11. EDS test area and results: (**a**) EDS test Results area 1; (**b**) EDS test Results area 2; (**c**) EDS test Results area 3; (**d**) EDS test Results area 4.

The EDS test results (Table 4) show that the location around the leak is rich in iron (Fe) and oxygen (O). The iron content has a value of 63.26% by weight to 75.27% by weight, and the oxygen content is 20.52% by weight to 30.82% by weight.

Table 4. EDS test results.

Location	Element								
	C	O	Na	Al	Si	S	Cl	Mn	Fe
a	2.33	24.83		0.45	0.85	0.33	1.91	0.39	68.85
b	2.18	20.52		0.24	0.26	0.23	0.64	0.66	75.27
c	2.94	28.83			0.45	0.27	1.94	0.36	65.20
d	3.3	30.82	0.21	0.30	0.46	0.46	0.76	0.44	63.25

SEM and EDS testing is also carried out on the cross sections of the pipe as shown in Figure 12. SEM and EDS were carried out in three areas. Area a is close to the leak point; area b is slightly far from the leak point; and area c is far from the leak point.

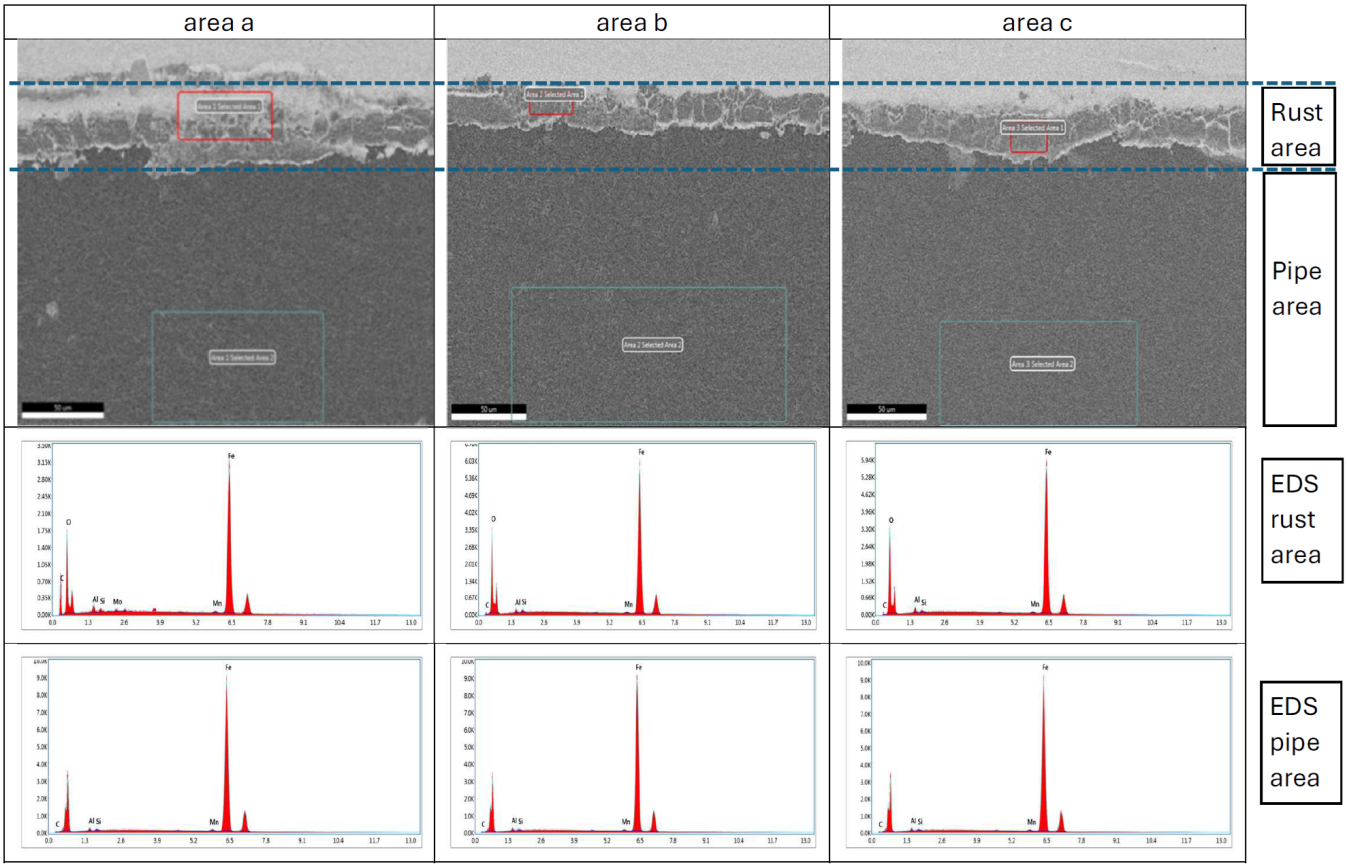

Figure 12. SEM and EDS Results on Pipe Cross Sections.

The crude oil transfer pipe from the GS BDA to the MGS A is an API 5L Grade B pipe, which has been confirmed through spectrometry testing. The crude oil transfer pipe from GS BDA to MGS A carries fluid in the form of a mixture of crude oil with a water cut of 50% (50% water content). The fluid flow in the pipe is stratified, with crude oil, which has a lower density, being above the produced water. Visual observation of the pipe samples showed differences in deposits in the top pipe (9 o'clock–3 o'clock direction) and deposits in the pipe (3 o'clock–9 o'clock direction).

FTIR test results show that the upper deposit is an aromatic compound as wax was formed during transfer of crude oil due to environment condition (1.5 m below the ground). While the bottom deposit characterization reveals main element of FeO_2 (Geothite), Fe_2O_3 (Hematite), and Fe_3O_4 (Magnetite) which further identified as corrosion products.

The test results for produced water containing sulphate-reducing bacteria (SRB) in SP BDA were 10^3–10^4, and in SPUA they were $<10^1$. The optimal temperature for SRB

growth is 40–110 °F (5–43 °C), with a maximum temperature limit of 120 °F (49 °C). The temperature of the formation water and crude oil at GS BDA is >141 °F (60 °C), so at this temperature, SRB cannot develop. Based on the SEM test results on the cross section of the pipe (Figure 11), no traces of pitting corrosion were found, so the corrosion that occurred was not caused by SRB.

The results of the produced water test show that the dissolved oxygen at the GS BDA was 3.96 ppm (3960 ppb) and the dissolved oxygen in the formation water at the MGS A was 1.37 ppm (1370 ppb), which means it is far above the limit level in API 571 (maximum 20 ppb) [16]. The dissolved oxygen causes corrosion on the surface of the pipe that is in contact with the produced water (3 o'clock–9 o'clock). The results of the produced water test showed that there was a chloride (Cl^-) content of 9968 mg/L at the GS BDA and 10,043 mg/L at the MGS A. SEM results (Figure 9) show that there are gaps on the corrosion surface. High chloride concentrations cause the movement of ions towards the bottom of the deposit through gaps in the deposit, resulting in under-deposit corrosion (UDC). The mechanism that occurs is a combination of oxygen corrosion and UDC, as follows:

a. Oxygen-Influenced Corrosion

The mechanism of Oxygen-Influenced Corrosion can be seen in Figure 13.

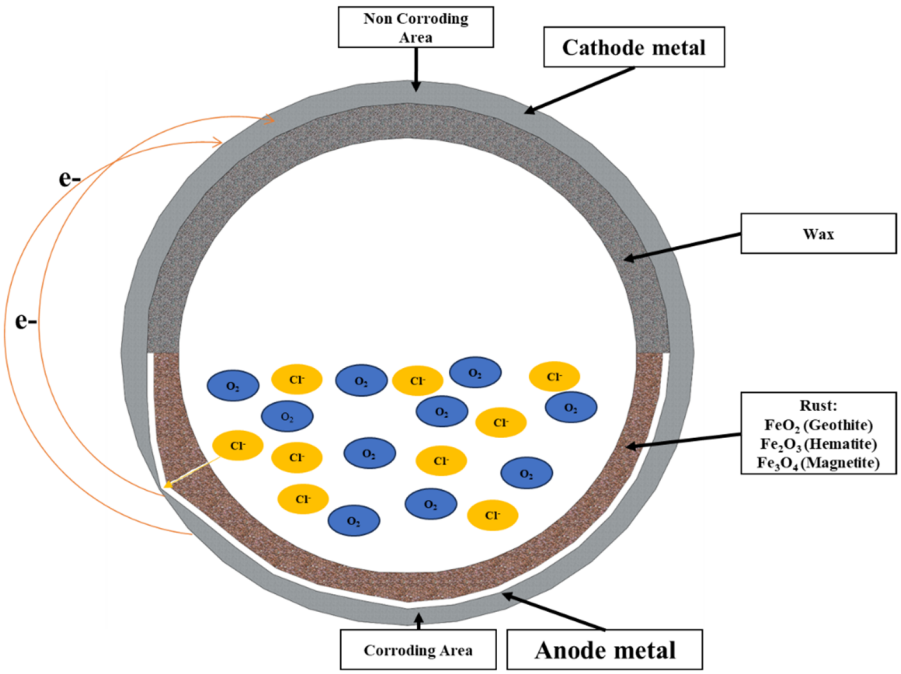

Figure 13. Oxygen-Influenced Corrosion Mechanisms.

In the anode area the following reaction occurs

$$Fe \rightarrow Fe^{2+} + 2e \quad (5)$$

In the cathode area, this occurs by reducing the oxygen in the produced water as follows:

$$O_2 + 2H_2O + 4e \rightarrow 4OH^- \quad (6)$$

At the anode, OH ions react with Fe^{2+} coming from the anode as follows:

$$Fe^{2+} + 2OH^- \rightarrow Fe(OH)_2 \quad (7)$$

With more access to oxygen in the produced water, $Fe(OH)_2$ oxidized to $Fe(OH)_3$ and then absorbs the water content:

$$4Fe(OH)_2 + O_2 + 2H_2O \rightarrow 4Fe(OH)_3 \quad (8)$$

Ferrous hydroxide is converted to hydrated ferric oxide or rust by oxygen:

$$4Fe(OH)_2 + O_2 \rightarrow 2Fe_2O_3.\ H_2O + 2H_2O \quad (9)$$

Fe_2O_3 reacts with $Fe(OH)_3{}^-$ as follows:

$$Fe_2O_3 + Fe(OH)_3{}^- \rightarrow Fe_3O_4 + H_2O + OH^- \quad (10)$$

b. Under Deposit Corrosion (UDC) mechanism

The Under Deposit Corrosion (UDC) mechanism can be seen in Figure 14.

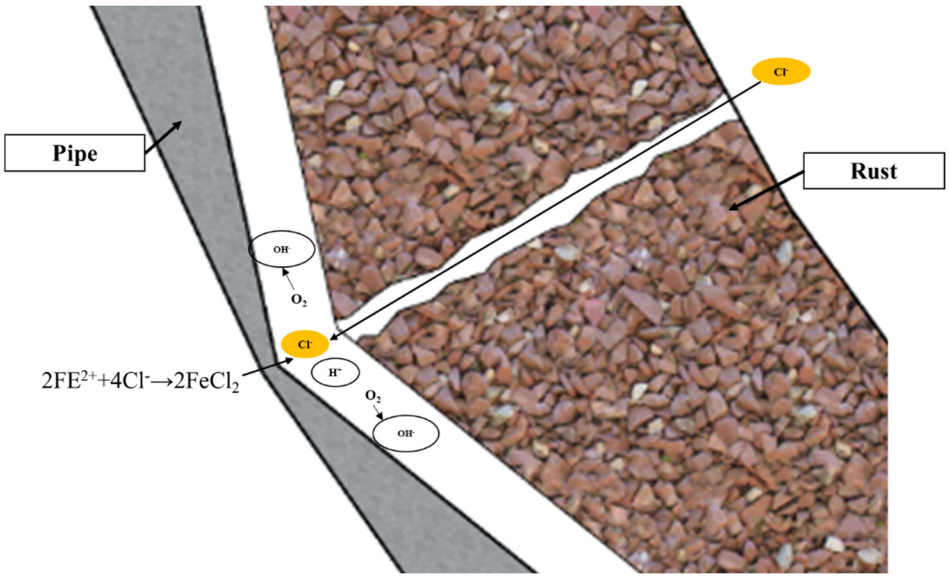

Figure 14. Under Deposit Corrosion (UDC) mechanism.

The formation of hydroxide ions (OH^-) causes the electrolyte under the deposit to have a more positive charge compared to the area above the deposit, causing chloride ions to enter under the deposit through the deposit gap to form $FeCl_2$ as follows:

$$2FE^{2+} + 4Cl^- \rightarrow 2FeCl_2 \quad (11)$$

$$4FE^{2+} + 12OH^- \rightarrow 4Fe(OH)_3 \quad (12)$$

$$2FeCl_2 + 4H_2O \rightarrow 2Fe(OH)_2 + 4H^+ + 4Cl^- \quad (13)$$

The $FeCl_2$ formed is hydrolyzed by water to form a weak base solution of $Fe(OH)_2$ and H^+ ions. H^+ ions have stronger acidic properties than the $Fe(OH)_2$ solution, so the area below the deposit experiences more rapid corrosion.

4. Conclusions

- Based on the spectometry test results, the crude oil transfer pipe can be confirmed to be an API 5L Grade B pipe.
- The main cause of pipe failure is under-deposit corrosion. Deposits are formed due to oxygen-influenced corrosion, which forms corrosion products. Corrosion products contain cracks that form gaps, causing chloride (Cl^-) to enter the deposit and causing under-deposit corrosion.

Author Contributions: Conceptualization, methodology, validation, formal analysis, investigation, writing—original draft preparation, writing—review and editing, supervision, project administration, funding acquisition, M. and F.M. All authors have read and agreed to the published version of the manuscript.

Funding: This research received no external funding.

Institutional Review Board Statement: Not applicable.

Informed Consent Statement: Not applicable.

Data Availability Statement: The data that support the findings of this study are available on request from the corresponding author. The data are not publicly available due to privacy or ethical restrictions.

Conflicts of Interest: The authors declare no conflict of interest.

References

1. Liu, T.; Chen, L.; Bi, H.; Che, X. Effect of Mo on high-temperature fatigue behavior of 15CrNbTi ferritic stainless steel. *Acta Metall. Sin. (Engl. Lett.)* **2014**, *27*, 452–456. [CrossRef]
2. Amadi, S.A. Analysis of corrosion induced failure of oil pipeline in the marine environment and possible control measures. *Jr. Ind. Pollut. Control* **2007**, *23*, 261–270.
3. Latypov, O.R.; Tyusenkov, A.S. Methodology for studying the corrosion of material of oilpipelines operating in marshy soil. *Mater. Sci. Eng.* **2020**, *962*, 042026.
4. Hamied, R.S.; Alhassan, M.A.; AL-Bidry, M.A. Study the Effect of Corrosion on the Pipes of Oil Well Production. *J. Pet. Res. Stud.* **2019**, *19*, E155–E164. [CrossRef]
5. Cheng, Y. Frank, Pipeline corrosion. *Corros. Eng. Sci. Technol.* **2015**, *50*, 161–162. [CrossRef]
6. Udonsek, D.E.; Tamonodukobipi, D.; Odokwo, V.E. Corrosion-Based Integrity Analysis of Offshore Pipeline for Hydrocarbon Transportation. *J. Power Energy Eng.* **2023**, *11*, 24–41.
7. Enani, J. Corrosion control in oil and gas pipelines. *Int. J. Sci. Eng. Res.* **2016**, *7*, 1161–1164.
8. Olabisi, O.T.; Chukwuka, A. Experimental Investigation of Pipeline Corrosion in a Polluted Niger Delta River. *Int. J. Oil Gas Coal Eng.* **2020**, *8*, 17–21. [CrossRef]
9. Li, J.; Sun, C.; Shuang, S.; Roostaei, M.; Fattahpour, V.; Mahmoudi, M.; Zeng, H.; Luo, J.L. Investigation on the flow-induced corrosion and degradation behavior of underground J55 pipe in a water production well in the Athabasca oil sands reservoir. *J. Pet. Sci. Eng.* **2019**, *182*, 106325. [CrossRef]
10. Martinez, S.; Mikšić, B.; Rogan, I.; Ivanković, A. *Inhibiting Corrosion in Transport Pipelines by VpCI Additives to Crude Oil*; Cortec Corporation: St. Paul, MN, USA, 2016; pp. 1–9.
11. American Petroleum Institut. *Specification for Line Pipe*; American Petroleum Institut: Washington, DC, USA, 2004.
12. Liu, H.S.; Duan, J.M.; Li, J.; Wang, J.; Yan, H.; Lin, K.Y.; Gu, K.C.; Li, C.J. Wax deposition modeling in oil-water stratified pipe flow. *Pet. Sci.* **2023**, *20*, 526–539. [CrossRef]
13. Olajire, A.A. Review of wax deposition in subsea oil pipeline systems and mitigation technologies in the petroleum industry. *Chem. Eng. J. Adv.* **2021**, *6*, 100104. [CrossRef]
14. Muhidin, D.; Rose, H.M. Stimulasi Thermochemical dan Electrical Downhole Heating sebagai Solusi Alternatif Penanganan Wax Problem pada Sumur High Pour Point Oil: Studi Kasus Lapangan "X". *J. Offshore Oil Prod. Facil. Renew. Energy* **2020**, *4*, 16–25. [CrossRef]
15. Nešić, S. Key issues related to modelling of internal corrosion of oil and gas pipelines—A review. *Corros. Sci.* **2007**, *49*, 4308–4338. [CrossRef]
16. *API RP 571*; Damage Mechanisms Affecting Fixed Equipment in the Refining Industry, 3rd ed. American Petroleum Institute: Washington, DC, USA, 2020.

Disclaimer/Publisher's Note: The statements, opinions and data contained in all publications are solely those of the individual author(s) and contributor(s) and not of MDPI and/or the editor(s). MDPI and/or the editor(s) disclaim responsibility for any injury to people or property resulting from any ideas, methods, instructions or products referred to in the content.